


# Oxygenation of the Mesoproterozoic ocean and the evolution of complex eukaryotes

Kan Zhang<sup>1,2</sup>, Xiangkun Zhu<sup>1\*</sup>, Rachel A. Wood<sup>3</sup>, Yao Shi<sup>1</sup>, Zhaofu Gao<sup>1</sup> and Simon W. Poulton<sup>1</sup> <sup>2</sup>

**The Mesoproterozoic era (1,600–1,000 million years ago (Ma)) has long been considered a period of relative environmental stasis, with persistently low levels of atmospheric oxygen. There remains much uncertainty, however, over the evolution of ocean chemistry during this period, which may have been of profound significance for the early evolution of eukaryotic life. Here we present rare earth element, iron-speciation and inorganic carbon isotope data to investigate the redox evolution of the 1,600–1,550 Ma Yanliao Basin, North China Craton. These data confirm that the ocean at the start of the Mesoproterozoic was dominantly anoxic and ferruginous. Significantly, however, we find evidence for a progressive oxygenation event starting at ~1,570 Ma, immediately prior to the occurrence of complex multicellular eukaryotes in shelf areas of the Yanliao Basin. Our study thus demonstrates that oxygenation of the Mesoproterozoic environment was far more dynamic and intense than previously envisaged, and establishes an important link between rising oxygen and the emerging record of diverse, multicellular eukaryotic life in the early Mesoproterozoic.**

The earliest definitive evidence for the evolution of eukaryotes occurs in late Paleoproterozoic marine sediments<sup>1,2</sup>, but the subsequent Mesoproterozoic has traditionally been perceived as a period of relative evolutionary stasis<sup>3</sup>. However, emerging evidence from several early Mesoproterozoic localities<sup>3–5</sup> increasingly supports a relatively high abundance and diversity of eukaryotic organisms by this time. Moreover, decimetre-scale multicellular fossils have recently been discovered in early Mesoproterozoic (~1,560 Ma) shelf sediments from the Gaoyuzhuang Formation of the Yanliao Basin, North China Craton<sup>6</sup>. Although their precise affinity is unclear, the Gaoyuzhuang fossils most probably represent photosynthetic algae, and provide the strongest evidence yet for the evolution of complex multicellular eukaryotes as early as the Mesoproterozoic<sup>6</sup>.

Although molecular oxygen is required for eukaryotic synthesis<sup>7</sup>, the precise oxygen requirements of early multicellular eukaryotes, which include the Gaoyuzhuang fossils, are unclear. This is exacerbated because recent reconstructions of oxygen levels across the Mesoproterozoic are highly variable, which has reignited the debate over the role of oxygen in early eukaryote evolution<sup>8–11</sup>. Thus, in addition to providing insight into the affinity of the Gaoyuzhuang fossils, a detailed understanding of the environmental conditions that prevailed in the Yanliao Basin would also inform on the nature of Earth surface oxygenation through the Mesoproterozoic.

Over recent years, our understanding of Mesoproterozoic ocean chemistry has converged on a scenario whereby the deep ocean remained predominantly anoxic and iron rich (ferruginous) beneath oxic surface waters, with widespread euxinic (anoxic and sulfidic) conditions being prevalent along biologically productive continental margins<sup>12–14</sup>. Other studies potentially indicate more variability in ocean redox during the Mesoproterozoic, with the suggestion that mid-depth waters may have become more oxygenated by ~1,400 Ma (refs. <sup>10,15,16</sup>). However, this possibility of an enhanced ocean oxygenation significantly postdates the occurrence of the Gaoyuzhuang fossils, and whether later Mesoproterozoic ocean oxygenation was

widespread remains unclear. Indeed, for surface waters in which photosynthetic eukaryotes had the potential to thrive, evidence from organic carbon isotopes on the North China Craton suggests a very shallow chemocline from ~1,650 to ~1,300 Ma (ref. <sup>17</sup>), and rare earth element (REE) data have been interpreted to reflect very low shallow water O<sub>2</sub> concentrations (~0.2 μM and below) throughout the Mesoproterozoic<sup>18</sup>.

Here we present REE, Fe-speciation and inorganic carbon isotope data for marine carbonates from the 1,600–1,550 Ma Yanliao Basin, to investigate ocean redox conditions in the basin where the Gaoyuzhuang fossils were discovered. Our data provide a more direct assessment of the potential links between the extent of environmental oxygenation and early eukaryote evolution, and suggest that the long-standing paradigm of the Mesoproterozoic as a period of prolonged environmental stasis requires conceptual reconsideration.

## Geological setting and samples

The Jixian Section in the Yanliao Basin, 100 km east of Beijing, China, preserves ~9 km thickness of Proterozoic sedimentary rocks deposited atop an Archean–Paleoproterozoic crystalline basement (Supplementary Information). Our samples were collected from the ~1,600–1,550 Ma Gaoyuzhuang Formation of the Jixian Section. The Gaoyuzhuang Formation is divided into four lithological members (Fig. 1), each of which comprises a shallowing-upward cycle that consists mainly of dolostone and limestone deposited in marine environments, which range from the deeper shelf slope to the supratidal/intertidal zone<sup>19,20</sup> (Fig. 1 and Supplementary Information give full details of the depositional setting). U–Pb dating of zircons from tuff beds in the lower and upper horizons of the Zhangjiayu Member of the Gaoyuzhuang Formation (Fig. 1) gives ages of 1,577 ± 12 Ma (ref. <sup>21</sup>) and 1,560 ± 5 Ma (ref. <sup>22</sup>), respectively.

## Evaluating ocean redox chemistry

With the exception of cerium (Ce), REEs are strictly trivalent in seawater and exhibit no intrinsic redox chemistry in most natural

<sup>1</sup>MLR Key Laboratory of Isotope Geology, MLR Key Laboratory of Deep-Earth Dynamics, Institute of Geology, Chinese Academy of Geological Sciences, Beijing, China. <sup>2</sup>School of Earth and Environment, University of Leeds, Leeds, UK. <sup>3</sup>School of Geosciences, University of Edinburgh, Edinburgh, UK.

\*e-mail: [xiangkunzhu@163.com](mailto:xiangkunzhu@163.com)

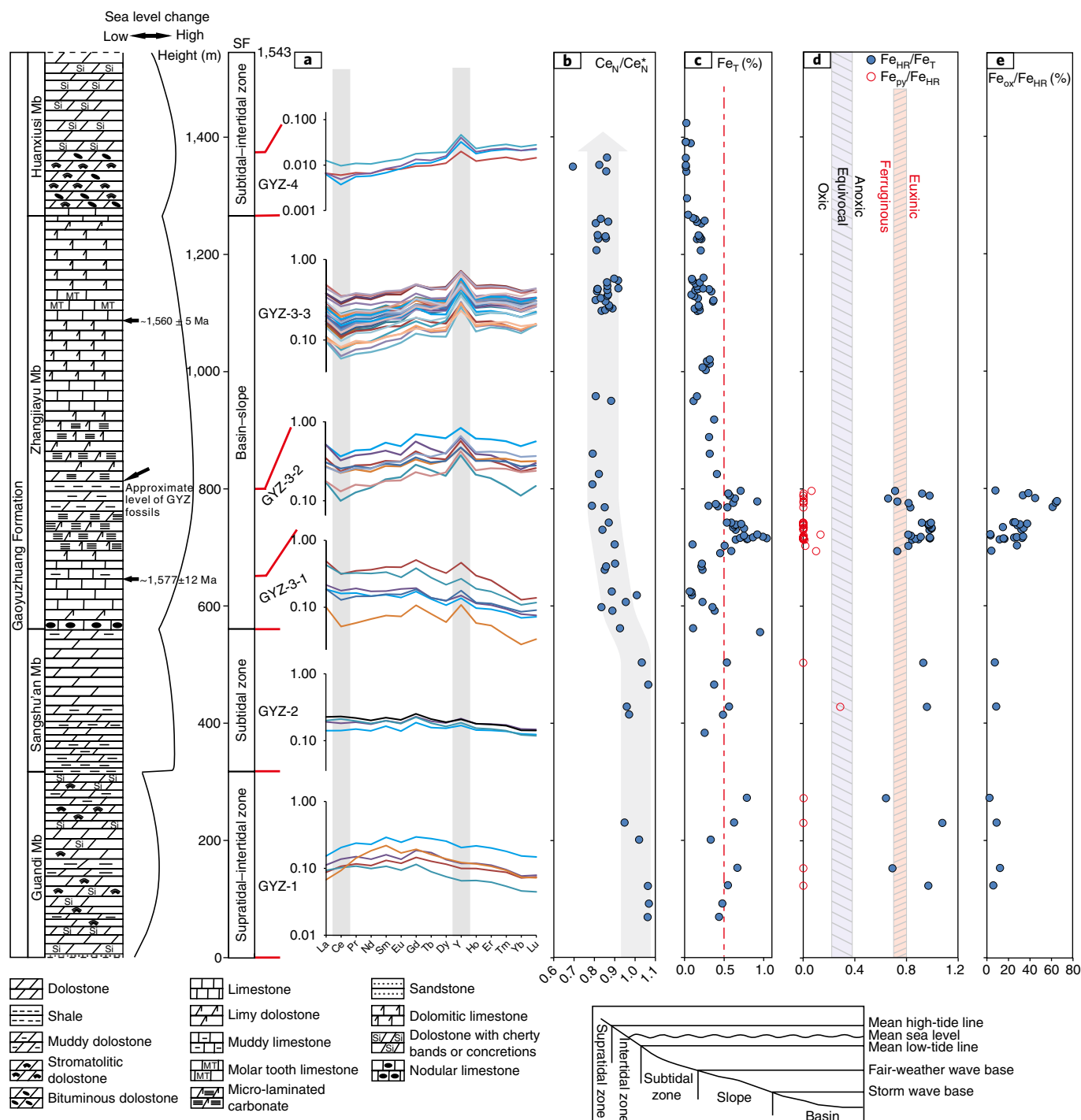


**Fig. 1 | Summary of sedimentary facies (SF) and geochemical signals for carbonates from the Gaoyuzhuang Formation, Jixian Section. a**, PAAS-normalized REE patterns categorized into six groups. **b**, Ce anomaly profile (Supplementary Information gives the calculation details). **c**,  $\text{Fe}_T$  profile (analytical precision is within the size of the symbols). **d**, Fe-speciation results (text gives the details). **e**,  $\text{Fe}_{\text{ox}}/\text{Fe}_{\text{HR}}$  profile. Sea level reached its highest around the middle Gaoyuzhuang Formation<sup>19,20</sup>. Mb, Member. Age data taken from refs<sup>21,22</sup>, and GYZ fossil level from ref.<sup>6</sup>.

waters (the reduction of europium (Eu) from Eu(III) to Eu(II) during magmatic, metamorphic or hydrothermal process is an exception<sup>23</sup>, but it is unlikely to have occurred in our samples). Solution complexation with ligands and surface adsorption to particles are fundamental processes that control REE cycling in aquatic environments<sup>24</sup>. REE-carbonate ion complexes are the dominant dissolved species in seawater, with a systematic increase in complexation behaviour that occurs from the light to the heavy REEs (HREEs)<sup>25</sup>.

Particulate organic matter and iron and manganese (oxyhydr) oxides are the dominant carriers of REEs, and the light REEs (LREEs) are preferentially scavenged by these particles compared to the HREEs<sup>24</sup>. These processes result in fractionation among the REEs, which leads to LREE depletion in oxic seawater<sup>24</sup>.

Yttrium (Y) and holmium (Ho) act as a twin pair due to their similar charge and radius. Silicate rocks or clastic sedimentary rocks generally have chondritic Y/Ho values of ~28, which implies no

apparent fractionation of Y from Ho (ref. <sup>26</sup>). By contrast, seawater is generally characterized by a superchondritic Y/Ho ratio (>44), which results from Ho being scavenged faster than Y (ref. <sup>27</sup>). The differential behaviour of Ce is particularly useful as a redox indicator of the water column. Ce exists in either a trivalent or a tetravalent form, and in oxygenated water soluble  $\text{Ce}^{3+}$  tends to adsorb to Fe and/or Mn (oxyhydr)oxide minerals on which oxidation to the highly insoluble  $\text{Ce}^{4+}$  is catalysed, which results in a negative Ce anomaly in the water column<sup>28</sup>. Therefore, compared to ambient oxic seawater, marine particulates generally have higher LREE/HREE ratios, lower Y/Ho ratios and smaller negative or even positive Ce anomalies<sup>24</sup>. When these particles settle into suboxic/anoxic deeper waters in a stratified ocean, REEs become involved in redox cycling, whereby particulate Mn, Fe and Ce undergo reductive dissolution, which releases scavenged trivalent REEs back into solution<sup>29</sup>. This generates higher LREE/HREE ratios, lower Y/Ho ratios and smaller negative or even positive Ce anomalies in the anoxic water column<sup>30,31</sup>. However, the original seawater REE patterns can be retained in coeval non-skeletal carbonates, and thus provide fundamental information on ocean redox conditions<sup>31</sup>.

Diagenetic alteration and non-carbonate contamination (for example, REEs in clay minerals) are two factors that require consideration prior to the interpretation of REE data<sup>32</sup>. However, carbonate REEs are generally robust to post-depositional process such as diagenesis or dolomitization<sup>33</sup>, and most samples evaluated in our study have experienced little diagenetic recrystallization and only very early dolomitization (based on petrographic features observed under optical microscopy and cathodoluminescence (Supplementary Information)). Although some dolomites from the fourth member of the Gaoyuzhuang Formation show a unimodal, non-planar texture that may reflect late burial dolomitization, these samples retain typical seawater-like REE patterns (Fig. 1a), which suggests little modification of the REE patterns. To address the potential for non-carbonate contamination, we utilized a sequential dissolution method for REEs using dilute acetic acid (Methods), which enables REEs in carbonates to be targeted specifically<sup>34</sup>. In addition, no obvious covariation was observed between aluminium (Al), scandium (Sc) or thorium (Th) (as indicators of detrital materials) and various REE parameters (for example, the sum of REEs ( $\Sigma\text{REE}$ ), Y/Ho ratios, the fractionation between LREE and HREE ( $\text{Pr}_{\text{N}}/\text{Er}_{\text{N}}$ ) or Ce anomalies ( $\text{Ce}_{\text{N}}/\text{Ce}_{\text{N}}^*$ ), where  $\text{REE}_{\text{N}}$  refers to observed PAAS-normalized REE abundance, and  $\text{REE}_{\text{N}}^*$  refers to predicted PAAS-normalized REE concentration) (Supplementary Fig. 5)). These observations provide strong support for the preservation and extraction of primary seawater REE signals<sup>32</sup>.

The post-Archean Australian Shale (PAAS)-normalized REE patterns of the Gaoyuzhuang Formation carbonates show systematic variability that can be categorized into six groups (Fig. 1a). Carbonates from ~0 to 650 m, including the Guandi Member, the Sangshu'an Member and the lower part of the Zhangjiayu Member of the Gaoyuzhuang Formation (Groups GYZ-1, GYZ-2 and GYZ-3-1), show marine REE patterns that are generally not typical of oxic seawater: middle REE enrichment, LREE enrichment or nearly flat REE patterns, near chondritic or slightly higher Y/Ho ratios and absent (or small) Ce anomalies. Samples from ~650 to 800 m (Group GYZ-3-2) show variable REE patterns, some of which start to show REE patterns and negative Ce anomalies typical of oxic seawater. Samples from 800 m to the top of the section (Group GYZ-3-3 and GYZ-4) show typical oxic marine REE patterns with negative Ce anomalies ( $\text{Ce}_{\text{N}}/\text{Ce}_{\text{N}}^* = 0.69\text{--}0.92$ ). These temporal trends in REE patterns record the long-term redox evolution of the Yanliao Basin.

In addition to the REE data, we also utilized Fe-speciation as an independent redox indicator. Fe-speciation is a well-calibrated technique to identify anoxia in the water column, and is the only

technique that enables ferruginous conditions to be distinguished directly from euxinia<sup>14,35</sup>. Besides its application to ancient fine-grained siliciclastic marine sediments, Fe-speciation can also be successfully applied to carbonate-rich sediments<sup>31,36,37</sup> provided the samples contain sufficient total Fe ( $\text{Fe}_{\text{T}} > 0.5 \text{ wt\%}$ ) to produce robust interpretations that are not skewed by the potential for Fe mobilization during late-stage diagenesis or deep burial dolomitization<sup>38</sup>. Hence, we only applied Fe-speciation to samples with  $\text{Fe}_{\text{T}} > 0.5 \text{ wt\%}$  (Fig. 1) and, in addition, our samples were screened for potential modification of primary signals by deep burial dolomitization (Supplementary Information).

Fe-speciation defines an Fe pool that is considered highly reactive ( $\text{Fe}_{\text{HR}}$ ) towards biological and abiological reduction under anoxic conditions, and includes carbonate-associated Fe ( $\text{Fe}_{\text{carb}}$ ), ferric oxides ( $\text{Fe}_{\text{ox}}$ ), magnetite ( $\text{Fe}_{\text{mag}}$ ) and pyrite ( $\text{Fe}_{\text{py}}$ )<sup>39</sup>. Sediments deposited from anoxic waters commonly have  $\text{Fe}_{\text{HR}}/\text{Fe}_{\text{T}} > 0.38$ , whereas ratios below 0.22 are generally considered to provide a robust indication of oxic depositional conditions<sup>14</sup>. For samples that show evidence of anoxic deposition (that is,  $\text{Fe}_{\text{HR}}/\text{Fe}_{\text{T}} > 0.38$ ), ferruginous conditions can be distinguished from euxinia by the extent of pyritization of the  $\text{Fe}_{\text{HR}}$  pool, with  $\text{Fe}_{\text{py}}/\text{Fe}_{\text{HR}} > 0.7\text{--}0.8$  indicating euxinia and  $\text{Fe}_{\text{py}}/\text{Fe}_{\text{HR}} < 0.7$  indicating ferruginous conditions<sup>35,40,41</sup>.

From 0 to 800 m in the Gaoyuzhuang Formation, 33 out of 54 samples had  $\text{Fe}_{\text{T}} > 0.5 \text{ wt\%}$  and were deemed suitable for Fe-speciation<sup>38</sup>, whereas all samples higher in the succession contained <0.5 wt% (Fig. 1c). The samples from 0 to 800 m show clear evidence for water-column anoxia, with high  $\text{Fe}_{\text{HR}}/\text{Fe}_{\text{T}} > 0.38$ . Furthermore, low  $\text{Fe}_{\text{py}}/\text{Fe}_{\text{HR}}$  ratios support ferruginous, rather than euxinic, depositional conditions (Fig. 1d). Fe-speciation also reveals a significant enrichment in ferric (oxyhydr)oxide minerals in GYZ-3-2 sediments, rather than reduced or mixed valence  $\text{Fe}_{\text{HR}}$  phases, with  $\text{Fe}_{\text{ox}}$  increasing up to 65% of the total  $\text{Fe}_{\text{HR}}$  pool (Fig. 1e), coincident with the first development of REE patterns typical of oxic seawater.

Carbonates were also analysed for their inorganic carbon isotope ( $\delta^{13}\text{C}_{\text{carb}}$ ) compositions. Values vary from  $-2.85\text{‰}$  to  $+0.54\text{‰}$  and are entirely consistent with previous analyses from other parts of the Yanliao Basin (Fig. 2). We interpret these  $\delta^{13}\text{C}_{\text{carb}}$  data to reflect contemporaneous seawater signatures with a minimal diagenetic overprint (Supplementary Information). Throughout much of the section there is a relatively narrow range in  $\delta^{13}\text{C}_{\text{carb}}$ , but a rapid, basin-wide, negative carbon isotope excursion (to values as low as  $-2.85\text{‰}$ ) occurs in the lower part of the Zhangjiayu Member of the Gaoyuzhuang Formation.

### Oxygenation of the early Mesoproterozoic ocean

Our REE and Fe-speciation data provide strong, independent evidence for anoxic depositional conditions across the lower two members, and the basal part of the Zhangjiayu Member, of the Gaoyuzhuang Formation (GYZ-1, GYZ-2 and GYZ-3-1 in Fig. 1). These samples span a significant range in water depth, from shallow to deeper distal environments<sup>19,20</sup>, which suggests that ferruginous conditions were a prevalent feature of the water column throughout the basin, including in very shallow waters (Fig. 3a). Above this, samples from ~650 to 800 m (GYZ-3-2 in Fig. 1) have variable REE features, which suggests precipitation around a transitional redox zone. In support of this, Fe-speciation data continue to record ferruginous conditions, which implies a redox boundary between the ferruginous deeper waters and shallower oxic waters. Moreover, an increase in the magnitude of negative Ce anomalies is apparent across this transitional zone (Fig. 1b), which also records a significant increase in the preservation of ferric (oxyhydr)oxide minerals in the sediment (Fig. 1e).

In combination, these observations suggest that our data capture a major transition in water-column oxygenation, which resulted in the extensive precipitation of Fe (oxyhydr)oxide minerals at the chemocline as ferruginous deeper waters became oxygenated (which

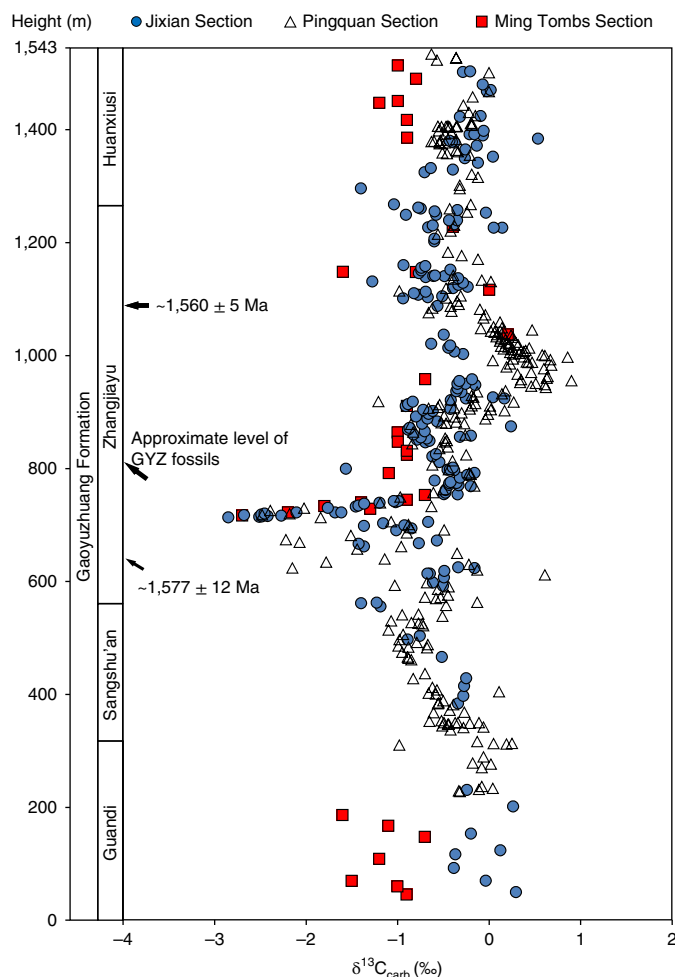


**Fig. 2 | Compilation of inorganic carbon isotope ( $\delta^{13}\text{C}_{\text{carb}}$ ) data for the Gaoyuzhuang Formation across the Yanliao Basin.** Data from the Jixian Section (this study), Pingquan Section<sup>44</sup> and Ming Tombs Section<sup>43</sup> (Supplementary Fig. 1a gives sample locations). Age data taken from refs <sup>21,22</sup>, and GYZ fossil level from ref. <sup>6</sup>. Analytical precision is within the size of the symbols.

is supported by the significant increase in  $\text{Fe}_T$  across this interval (Fig. 1c). Indeed, this transitional redox zone occurs as the water depth increases to almost the maximum observed in the succession (Fig. 1), which suggests that a significant rise in surface-water oxygen levels resulted in a major deepening of the chemocline, as depicted in Fig. 3b.

REE systematics then support the persistence of well-oxygenated waters throughout the overlying succession, from deep basinal waters, through fluctuating water depths, to very shallow waters. If the dissolved oxygen content remained constant as the water depth shallowed through time, a change from more negative (in deeper waters) to less negative (in shallower waters) Ce anomalies would naturally occur, due to the preferential desorption of LREEs relative to Ce(IV) at depth in the water column<sup>42</sup>. Therefore, the relatively stable negative Ce anomalies (and the one sample with a large negative anomaly) as water depth shallows from 800 m to the top of the Gaoyuzhuang Formation (Fig. 1b) imply a continued progressive oxygenation of the water column (Fig. 3c). The very low  $\text{Fe}_T$  content of these samples after the large-scale drawdown of water-column Fe in unit GYZ-3-2 (Fig. 1) is also entirely consistent with an absence of  $\text{Fe}_{\text{HR}}$  (and  $\text{Fe}_{\text{py}}$ ) enrichments due to persistent water-column oxygenation<sup>38</sup>.

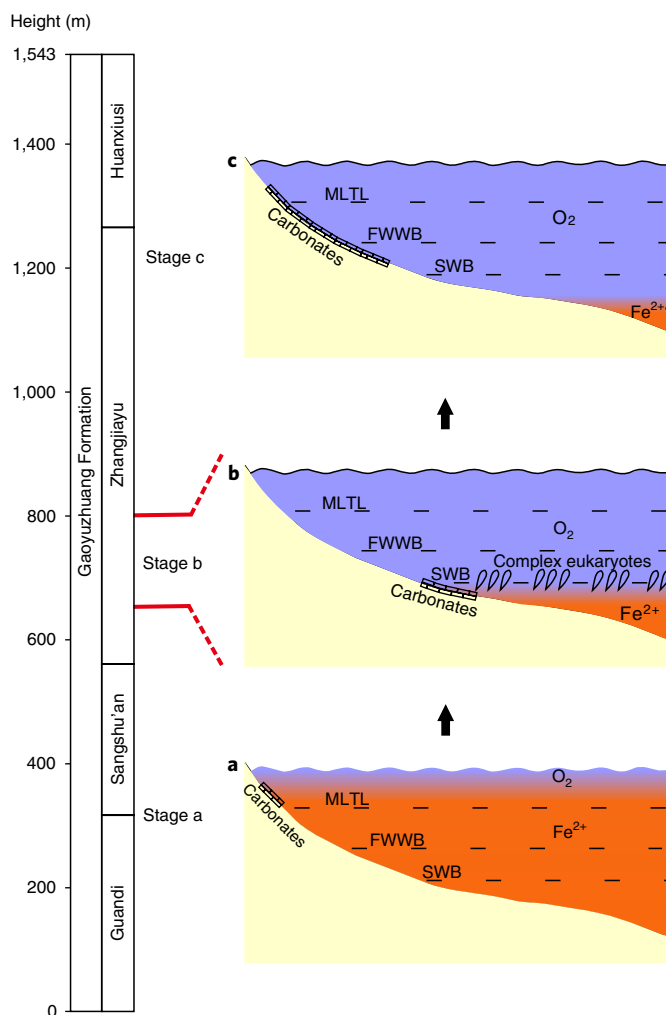


**Fig. 3 | Depiction of the redox evolution in the early Mesoproterozoic Yanliao Sea.** Three stages are illustrated along with the relative position of carbonates analysed for this study. **a**, In the earliest Mesoproterozoic, seawater was anoxic and ferruginous with a very shallow chemocline. **b**, The chemocline deepened, probably to below the SWB (storm wave base), around the middle of Gaoyuzhuang Formation in response to the onset of oxygenation. The increase in shallow-water oxygenation coincides with the presence of decimetre-scale complex multicellular eukaryotes. **c**, The extent of the ocean oxygenation continued to increase with time. MLTL, mean low-tide line; FWWB, fair-weather wave base.

Our reconstruction of anoxic ferruginous water-column conditions in very shallow waters of the lower Gaoyuzhuang Formation (Fig. 3a) is consistent with previous studies that suggest a very low surface-water oxygenation in the Mesoproterozoic<sup>17</sup>. However, we also find clear evidence for a progressive oxygenation ‘event’ beginning at ~1,570 Ma. REE and Fe-speciation data are, however, considered to record local to regional water-column redox conditions. To place our observations in the more widespread context of the entire Yanliao Basin, we also consider carbon isotope systematics from the Jixian Section and elsewhere in the basin. A prominent negative  $\delta^{13}\text{C}_{\text{carb}}$  excursion, lasting ~1.6 Myr (assuming a constant depositional rate), is apparent throughout the Yanliao Basin at ~1,570 Ma (Fig. 2), coincident with the onset of the oxygenation event, as recorded independently by our geochemical data. This excursion was previously attributed to diagenetic alteration<sup>43</sup>, but more-detailed isotopic studies suggested that the excursion reflects the development of anoxic bottom waters in deeper basinal



environments, which may have resulted in an enhanced heterotrophic remineralization under anoxic conditions<sup>19</sup>. However, these previous studies lacked the environmental context afforded by our redox evaluation of the water column, which suggests that, by contrast, the excursion is linked to the development of oxic, rather than anoxic, conditions.

Based on our data, we consider two potential mechanisms to explain the negative  $\delta^{13}\text{C}_{\text{carb}}$  excursion. One mechanism requires a widespread decline in organic carbon burial, but this is inconsistent with the total organic carbon data, which show an increase from <0.1 wt% below the excursion to ~0.5 wt% during the excursion (Supplementary Fig. 7). Instead, we suggest that the negative  $\delta^{13}\text{C}_{\text{carb}}$  excursion is directly related to widespread oxygenation in the basin, and probably reflects the oxidation of a  $\delta^{13}\text{C}$ -depleted pool of dissolved organic carbon and/or methane at the redoxcline. The  $\delta^{13}\text{C}_{\text{carb}}$  record of early Mesoproterozoic successions in the Yanliao Basin also shows a gentle long-term increase to more-positive values above the negative isotope excursion (Fig. 2)<sup>44</sup>, which is also consistent with the progressive longer-term increase in oxygenation indicated by our REE data. This is consistent with the emerging evidence for a possible deeper water oxygenation recorded in marine sediments from the ~1,400 Ma Kaltasy Formation (Russia)<sup>16</sup>, and in the ~1,400–1,320 Ma Xiamaling Formation (North China)<sup>10,15</sup>. These observations suggest that our data may capture the onset of a major global rise in Mesoproterozoic Earth surface oxygenation, which contrasts with the persistent low-oxygen condition often advocated for this period<sup>8,9,17,18</sup>.

### Implications for eukaryote evolution

The complex eukaryotes of the Gaoyuzhuang Formation (Fig. 1) are found in the Zhangjiayu Member<sup>6</sup>, shortly after the onset of the oxygenation event recorded by our geochemical data. In addition, the Gaoyuzhuang fossils are found near the storm wave base (SWB) on the shelf (Fig. 3b)<sup>6</sup>, which suggests that rising oxygen levels and a concomitant deepening of the oxycline created the environmental stability required for their evolution. This reinforces the role of oxygen as an evolutionary driver in the Mesoproterozoic, and provides support for the suggestion that these complex eukaryotes were probably involved in aerobic respiration and photosynthesis<sup>6</sup>. Although Gaoyuzhuang-type fossils have not yet been discovered elsewhere, several other early Mesoproterozoic successions, including the Ruyang Group (~1,750–1,400 Ma) in the southwestern margin of the North China Craton<sup>3</sup>, the Kotuikan Formation (~1,500 Ma) on the northern Siberia Platform<sup>5</sup> and the Roper Group (~1,500 Ma) in northern Australia<sup>4</sup>, have been reported to preserve a relatively high abundance and diversity of eukaryotic organisms, in contrast to older strata. This suggests that chemical and biological evolution during the Mesoproterozoic were probably intrinsically linked, and far from static, on a global scale.

In summary, the early Mesoproterozoic Yanliao Basin records an important step change in Earth's oxygenation history, which was most probably linked to atmospheric oxygenation. The emerging evidence from the North China Craton and elsewhere<sup>10,15,16</sup> suggests that the progressive oxygenation event recorded by our data may have been of global significance, with major implications for eukaryote evolution. Although further detailed study of other successions is required to evaluate the spatial and temporal constraints on early Mesoproterozoic oxygenation, our data build upon emerging evidence from the fossil record to suggest that environmental change was probably considerably more dynamic than previously recognized during the far from 'boring' Mesoproterozoic Era.

### Methods

Methods, including statements of data availability and any associated accession codes and references, are available at <https://doi.org/10.1038/s41561-018-0111-y>.

Received: 24 September 2017; Accepted: 22 March 2018;  
Published online: 23 April 2018

### References

- Rasmussen, B., Fletcher, I. R., Brocks, J. J. & Kilburn, M. R. Reassessing the first appearance of eukaryotes and cyanobacteria. *Nature* **455**, 1101–1104 (2008).
- Knoll, A. H., Javaux, E. J., Hewitt, D. & Cohen, P. Eukaryotic organisms in Proterozoic oceans. *Philos. Trans. R. Soc. Lond. B* **361**, 1023–1038 (2006).
- Agic, H., Moczydlowska, M. & Yin, L. Diversity of organic-walled microfossils from the early Mesoproterozoic Ruyang Group, North China Craton—a window into the early eukaryote evolution. *Precambrian Res.* **297**, 101–130 (2017).
- Javaux, E. J., Knoll, A. H. & Walter, M. R. Morphological and ecological complexity in early eukaryotic ecosystems. *Nature* **412**, 66–69 (2001).
- Vorobeva, N. G., Sergeev, V. N. & Petrov, P. Y. Kotuikan Formation assemblage: a diverse organic-walled microbiota in the Mesoproterozoic Anabar succession, northern Siberia. *Precambrian Res.* **256**, 201–222 (2015).
- Zhu, S. et al. Decimetre-scale multicellular eukaryotes from the 1.56-billion-year-old Gaoyuzhuang Formation in North China. *Nat. Commun.* **7**, 11500 (2016).
- Summons, R. E., Bradley, A. S., Jahnke, L. L. & Waldbauer, J. R. Steroids, triterpenoids and molecular oxygen. *Philos. Trans. R. Soc. Lond. B* **361**, 951–968 (2006).
- Lyons, T. W., Reinhard, C. T. & Planavsky, N. J. The rise of oxygen in Earth's early ocean and atmosphere. *Nature* **506**, 307–315 (2014).
- Planavsky, N. J. et al. Low Mid-Proterozoic atmospheric oxygen levels and the delayed rise of animals. *Science* **346**, 635–638 (2014).
- Zhang, S. et al. Sufficient oxygen for animal respiration 1,400 million years ago. *Proc. Natl Acad. Sci. USA* **113**, 1731–1736 (2016).
- Daines, S. J., Mills, B. J. & Lenton, T. M. Atmospheric oxygen regulation at low Proterozoic levels by incomplete oxidative weathering of sedimentary organic carbon. *Nat. Commun.* **8**, 14379 (2017).
- Poulton, S. W., Fralick, P. W. & Canfield, D. E. Spatial variability in oceanic redox structure 1.8 billion years ago. *Nat. Geosci.* **3**, 486–490 (2010).
- Planavsky, N. J. et al. Widespread iron-rich conditions in the mid-Proterozoic ocean. *Nature* **477**, 448–451 (2011).
- Poulton, S. W. & Canfield, D. E. Ferruginous conditions: a dominant feature of the ocean through Earth's history. *Elements* **7**, 107–112 (2011).
- Wang, X. et al. Oxygen, climate and the chemical evolution of a 1400 million year old tropical marine setting. *Am. J. Sci.* **317**, 861–900 (2017).
- Sperling, E. A. et al. Redox heterogeneity of subsurface waters in the Mesoproterozoic ocean. *Geobiology* **12**, 373–386 (2014).
- Luo, G. et al. Shallow stratification prevailed for ~1700 to ~1300 Ma ocean: evidence from organic carbon isotopes in the North China Craton. *Earth Planet. Sci. Lett.* **400**, 219–232 (2014).
- Tang, D., Shi, X., Wang, X. & Jiang, G. Extremely low oxygen concentration in mid-Proterozoic shallow seawaters. *Precambrian Res.* **276**, 145–157 (2016).
- Guo, H. et al. Sulfur isotope composition of carbonate-associated sulfate from the Mesoproterozoic Jixian Group, North China: implications for the marine sulfur cycle. *Precambrian Res.* **266**, 319–336 (2015).
- Mei, M. Preliminary study on sequence-stratigraphic position and origin for molar-tooth structure of the Gaoyuzhuang Formation of Mesoproterozoic at Jixian section in Tianjin. *J. Palaeogeogr.* **7**, 437–447 (2005).
- Tian, H. et al. Zircon LA-MC-ICPMS U–Pb dating of tuff from Mesoproterozoic Gaoyuzhuang Formation in Jixian Country of North China and its geological significance. *Acta Geosci. Sin.* **36**, 647–658 (2015).
- Li, H. et al. Further constraints on the new subdivision of the Mesoproterozoic stratigraphy in the northern North China Craton. *Acta Petrol. Sin.* **26**, 2131–2140 (2010).
- Michard, A., Albarède, F., Michard, G., Minster, J. F. & Charlou, J. L. Rare-earth elements and uranium in high-temperature solutions from East Pacific Rise hydrothermal vent field (13 °N). *Nature* **303**, 795–797 (1983).
- Sholkovitz, E. R., Landing, W. M. & Lewis, B. L. Ocean particle chemistry: the fractionation of rare earth elements between suspended particles and seawater. *Geochim. Cosmochim. Acta* **58**, 1567–1579 (1994).
- Cantrell, K. J. & Byrne, R. H. Rare earth element complexation by carbonate and oxalate ions. *Geochim. Cosmochim. Acta* **51**, 597–605 (1987).
- Bau, M. Controls on the fractionation of isoivalent trace elements in magmatic and aqueous systems: evidence from Y/Ho, Zr/Hf, and lanthanide tetrad effect. *Contrib. Mineral. Petrol.* **123**, 323–333 (1996).
- Nozaki, Y., Zhang, J. & Amakawa, H. The fractionation between Y and Ho in marine environment. *Earth Planet. Sci. Lett.* **148**, 329–340 (1997).
- Bau, M. & Koschinsky, A. Oxidative scavenging of cerium on hydrous Fe oxides: evidence from the distribution of rare earth elements and yttrium between Fe oxides and Mn oxides in hydrogenetic ferromanganese crusts. *Geochim. J.* **43**, 37–47 (2009).

29. German, C. R., Holliday, B. P. & Elderfield, H. Redox cycling of rare earth elements in the suboxic zone of the Black Sea. *Geochim. Cosmochim. Acta*. **55**, 3553–3558 (1991).
30. Bau, M., Moller, P. & Dulski, P. Yttrium and lanthanides in eastern Mediterranean seawater and their fractionation during redox-cycling. *Mar. Chem.* **56**, 123–131 (1997).
31. Tostevin, R. et al. Low-oxygen waters limited habitable space for early animals. *Nat. Commun.* **7**, 12818 (2016).
32. Nothdurft, L. D., Webb, G. E. & Kamber, B. S. Rare earth element geochemistry of Late Devonian reefal carbonates, Canning Basin, Western Australia: confirmation of a seawater REE proxy in ancient limestones. *Geochim. Cosmochim. Acta*. **68**, 263–283 (2004).
33. Banner, J. L., Hanson, G. N. & Meyers, W. J. Rare earth elements and Nd isotopic variations in regionally extensive dolomites from the Burlington–Keokuk Formation (Mississippian): implications for REE mobility during carbonate diagenesis. *J. Sediment. Petrol.* **58**, 415–432 (1988).
34. Zhang, K., Zhu, X. & Yan, B. A refined dissolution method for rare earth element studies of bulk carbonate rocks. *Chem. Geol.* **412**, 82–91 (2015).
35. Poulton, S. W., Fralck, P. W. & Canfield, D. E. The transition to a sulphidic ocean ~1.84 billion years ago. *Nature* **431**, 173–177 (2004).
36. Clarkson, M. O. et al. Dynamic anoxic ferruginous conditions during the end-Permian mass extinction and recovery. *Nat. Commun.* **7**, 12236 (2016).
37. Wood, R. A. et al. Dynamic redox conditions control late Ediacaran metazoan ecosystems in the Nama Group, Namibia. *Precambrian Res.* **261**, 252–271 (2015).
38. Clarkson, M. O., Poulton, S. W., Guilbaud, R. & Wood, R. A. Assessing the utility of Fe/Al and Fe-speciation to record water column redox conditions in carbonate-rich sediments. *Chem. Geol.* **382**, 111–122 (2014).
39. Poulton, S. W. & Canfield, D. E. Development of a sequential extraction procedure for iron: implications for iron partitioning in continentally derived particulates. *Chem. Geol.* **214**, 209–221 (2005).
40. Poulton, S. W. & Raiswell, R. The low-temperature geochemical cycle of iron: from continental fluxes to marine sediment deposition. *Am. J. Sci.* **302**, 774–805 (2002).
41. Raiswell, R. & Canfield, D. E. Sources of iron for pyrite formation in marine sediments. *Am. J. Sci.* **298**, 219–245 (1998).
42. Ling, H. et al. Cerium anomaly variations in Ediacaran–earliest Cambrian carbonates from the Yangtze Gorges area, South China: implications for oxygenation of coeval shallow seawater. *Precambrian Res.* **225**, 110–127 (2013).
43. Li, R., Chen, J., Zang, S. & Chen, Z. Secular variations in carbon isotopic compositions of carbonates from Proterozoic successions in the Ming Tombs Section of the North China Platform. *J. Asian Earth Sci.* **22**, 329–341 (2003).
44. Guo, H. et al. Isotopic composition of organic and inorganic carbon from the Mesoproterozoic Jixian Group, North China: implications for biological and oceanic evolution. *Precambrian Res.* **224**, 169–183 (2013).

## Acknowledgements

This work was supported by NSFC Grant 41430104 and CAGS Research Fund YYWF201603 to X.K.Z., a China Scholarship Council award to K.Z. and a China Geological Survey Grant DD20160120-04 to B. Yan. S.W.P. acknowledges support from a Royal Society Wolfson Research Merit Award. We thank L. Gao and P. Liu for field guidance, and F. Shi, C. Tang, X. Peng, C. Pan, N. Zhao, C. Bao, Z. Zhou, F. Zhang and Y. Guo for field-work assistance. We acknowledge F. Xu and M. Lv for assistance in the elemental analysis, Y. Xiong for help with the Fe-speciation experiments, Y. Shen, K. Chen and W. Huang for carbon isotope analyses and F. Bowyer for assistance with cathodoluminescence. We also express our thanks to J. Li, D. Li, Y. He, J. Ma, X. Zou and K. Du for logistical support.

## Author contributions

X.K.Z. designed the project. X.K.Z., K.Z., Y.S. and Z.F.G. did the fieldwork and collected samples. K.Z. carried out the elemental and Fe-speciation analyses. R.A.W. provided expertise in the evaluation of carbonate diagenesis. X.K.Z., K.Z. and S.W.P. interpreted the data, and K.Z., S.W.P. and X.K.Z. wrote the paper, with additional input from all the co-authors.

## Competing interests

The authors declare no competing interests.

## Additional information

**Supplementary information** is available for this paper at <https://doi.org/10.1038/s41561-018-0111-y>.

**Reprints and permissions information** is available at [www.nature.com/reprints](http://www.nature.com/reprints).

**Correspondence and requests for materials** should be addressed to X.Z.

**Publisher's note:** Springer Nature remains neutral with regard to jurisdictional claims in published maps and institutional affiliations.

## Methods

**REEs.** The chemical dissolution of REEs was carried out in a class 100 ultraclean laboratory. The dissolution method applied is reported elsewhere<sup>34</sup>. Briefly, the technique initially dissolves 30–40% of total carbonate, followed by a subsequent extraction of the next 30–40% of total carbonate using dilute acetic acid (0.5 mol/l), which was sampled for REEs and considered to best represent that of the carbonate source water. Elemental analysis, including REEs, Th, Sc, Ca, Mg and Al in carbonate leachates, was conducted via inductively coupled plasma mass spectrometry and inductively coupled plasma optical emission spectrometry, with replicate extractions that gave a relative standard deviation (RSD) of less than 3% for these elements.

**Fe-speciation and Fe<sub>T</sub>.** Fe-speciation extraction was performed using standard sequential extraction protocols<sup>39</sup>. Fe<sub>carb</sub> was extracted with a sodium acetate solution at pH 4.5 for 48 h at 50 °C, Fe<sub>ox</sub> was then extracted with a sodium dithionite solution at pH 4.8 for 2 h at room temperature and, finally, Fe<sub>mag</sub> was extracted with an ammonium oxalate solution for 6 h at room temperature. All the Fe concentrations were measured via atomic absorption spectrometry (AAS) with replicate extractions that gave a RSD of <5% for all the phases. Fe<sub>T</sub> was determined by one of two methods: (1) X-ray fluorescence and (2) a HNO<sub>3</sub>–HF–HClO<sub>4</sub> digest on ashed samples (overnight at 550 °C) followed by AAS analysis.

Fe<sub>py</sub> was calculated on the basis of the weight percentage of sulfur extracted during chromous chloride distillation<sup>45</sup>, with a RSD of <5%.

**Inorganic carbon isotopes.** To determine  $\delta^{13}\text{C}_{\text{carb}}$ , carbonate powders of ~150 µg were first reacted with anhydrous phosphoric acid at 70 °C to extract CO<sub>2</sub> using a KEIL IV carbonate device. The produced CO<sub>2</sub> was then purified stepwise and ultimately introduced into a Finnigan MAT 253 mass spectrometer. Carbon isotope determinations were performed using a dual-inlet mode against an in-house standard reference gas in the mass spectrometer. All the values are reported as  $\delta^{13}\text{C}_{\text{carb}}$  relative to the Vienna Pee Dee Belemnite standard. The precision is better than 0.06‰ based on replicate analyses of the Chinese national standard GBW04416 ( $\delta^{13}\text{C} = 1.61 \pm 0.03\text{‰}$ ).

**Data availability.** The authors declare that the data supporting the findings of this study are available within the article and its supplementary information files.

## References

45. Canfield, D. E., Raiswell, R., Westrich, J. T., Reaves, C. M. & Berner, R. A. The use of chromium reduction in the analysis of reduced inorganic sulfur in sediments and shales. *Chem. Geol.* **54**, 149–155 (1986).